

Multiple scattering of light in porous glass

Sakae Kawato, Toshiaki Hattori, Tadashi Takemori, and Hiroki Nakatsuka
Institute of Applied Physics, University of Tsukuba, Tsukuba, Ibaraki 305, Japan

(Received 29 June 1993)

Two kinds of multiple-light-scattering measurements were performed for porous glass plates of several pore radii from 0.15 to 0.50 μm . One is the measurement of the angular dependence of the backscattered light intensity, and the other is the measurement of the temporal profile of light pulses transmitted through the sample. The measured curves were in very good agreement with the theoretical ones based on the diffusion model in uniform scattering media, and no features specific to the local geometry of porous glass were found. The pore radius dependence of the transport mean free path l^* could be explained well by a Mie scattering calculation based on the independent scattering approximation. The transport velocity of light in the porous glasses in the measured range of the pore size calculated from the obtained values of l^* and the diffusion constants was around 60% of the phase velocity in the bulk glass.

I. INTRODUCTION

Recently there has been much interest in the multiple scattering of light in random media and its relationship with Anderson localization, since the enhanced backscattering was found to be a manifestation of the weak localization of light.^{1,2} It has been shown that scattered light intensity in the exact backscattering direction is enhanced by a factor of 2, and that the width of the peak is on the order of λ/l^* , where l^* is the transport mean free path and λ is the wavelength of light. Although the strong localization of light has been found to be difficult to achieve,³ studies of the intensity and the shape of the backscattering peak can reveal the transport properties of light in the spatial scale of l^* in inhomogeneous media.

Several experimental studies on the multiple scattering of light have been reported so far by measuring the backscattering peak shape or using other methods such as measurements of the time-of-flight profile⁴ and of total transmission.⁵ Almost all the measurements, however, have been limited to scattering media with spherically shaped scatterers, such as polystyrene latex and corpuscles of BaSO_4 or TiO_2 .¹⁻⁷ In the experiment of multiple light scattering, the generally expected features, which the target sample should have are well-characterized spatial structures, controllability of the size of the scatterers, low light loss, and high contrast of the refractive indices between the host and the scatterers. It is known that the distribution of the pore radius of porous glass can be controlled within $\pm 10\%$ around the mean value, and the mean pore radius and the volume fraction of pore can be measured precisely. Therefore, we were interested in porous glass as a well-characterized low-light-loss sample that has a different spatial structure from previously studied samples. Moreover, it is reported that the structure of porous glasses has a fractal nature.^{8,9} It is of great interest how the fractal dimensionality of the scattering media affects the multiple scattering properties of light.

In the present paper, the multiple scattering of light in porous glasses was studied by two kinds of measure-

ments. One is the measurement of the angular dependence of the intensity of the backscattered light, and the other is the measurement of the temporal profile of a light pulse transmitted through the sample. The transport mean free paths l^* and the diffusion constants D of light in the samples were obtained from these measurements, respectively, and the transport velocities of light were calculated using the Boltzmann relation. Four samples of porous glass plates [Asahi Glass, MPG-AM(S)] with different pore radii were studied in the measurements. They were *A* (mean pore radius $r=0.15 \mu\text{m}$, volume fraction of pore $f=0.53$), *B* ($r=0.275 \mu\text{m}$, $f=0.50$), *C* ($r=0.35 \mu\text{m}$, $f=0.49$), and *D* ($r=0.50 \mu\text{m}$, $f=0.48$), and their thicknesses were 0.5 mm.

II. BACKSCATTERING MEASUREMENTS

In the backscattering measurement, a linearly polarized collimated beam at 514.5 nm from a cw Ar-ion laser was reflected by a beam splitter and incident on the sample plate with a small angle from the normal incidence. The scattered light around the backscattering direction was transmitted through the beamsplitter and focused by a lens with a focal length of 210 mm. A 50- μm pinhole was scanned in the focal plane of the lens in the direction perpendicular to the polarization of the laser light, and the intensity of the scattered light with the polarization parallel to the incident light polarization was detected by a photomultiplier tube. The sample was rotated around the axis normal to the sample surface at about 10 Hz in order to average out speckles. The obtained backscattering intensities are shown by dots in Fig. 1 as a function of the angle from the exact backscattering direction. The intensities are normalized to the incoherent portion intensity obtained by the fitting procedure described below. The resolution curve of the measurement, which is shown at the bottom of the figure, was obtained by replacing the sample by a plane mirror, which was set normal to the incident beam. The full width at half maximum of the resolution curve was 0.6 mrad, which was much smaller

than the widths of the backscattering peaks. The transport mean free paths of light in the samples were obtained by fitting the data to the convolution of the resolution curve and the theoretical curve based on the diffusion of vector wave in media with uniformly distributed isotropic scatterers.^{10,11} According to the theory, the angle dependence of the backscattered light intensity

is composed of an angle-independent incoherent portion and a peak-shaped coherent portion. The coherent portion, $J_{\text{coh}}(\theta)$, is expressed as

$$J_{\text{coh}}(\theta) = I(\theta, \infty) + 2I(\theta, (\sqrt{7}/3)l^*), \quad (1)$$

where, $I(\theta, \xi)$ is defined by

$$I(\theta, \xi) \equiv \frac{1}{2\pi l^{*3}} \int_0^W dz_+ \int_0^W dz_- e^{-z_+/l^*} e^{-z_-/l^*} \int_{\rho} d^2\rho e^{-i\rho q} \sum_n \left[\frac{e^{-(\rho^2 + a_n^2)^{1/2}/\xi}}{(\rho^2 + a_n^2)^{1/2}} - \frac{e^{-(\rho^2 + b_n^2)^{1/2}/\xi}}{(\rho^2 + b_n^2)^{1/2}} \right]. \quad (2)$$

Here, θ and W are the angle of the scattered light from the backscattering direction and the thickness of the sample, respectively, $q = 2k \sin(\theta/2)$ is the scattering wave vector,

$$a_n = z_+ - z_- + 2n(W + 2z_0)$$

and

$$b_n = z_+ + z_- + 2z_0 + 2n(W + 2z_0).$$

The overall amplitude of the coherent portion and l^* were the variable parameters in the fitting, and the effect of absorption of light was not taken into account. The value of z_0 was set to $0.7104l^*$. The solid lines in the figure are the fitting curves. The measured curves agree very well with the theoretical ones.

The fractal nature of the surface structure of porous glasses has been revealed by studies on the dynamics of energy transfer between dyes adsorbed on porous glasses,⁸ and by analyses of x-ray and neutron scattering.⁹ The multiple scattering of light in such media is also affected by the fractal geometry, and the shape of the backscattering peak can be different from the three-dimensional one. The shape of the backscattering peak from scattering media with a fractal dimension has been studied by Akkermans *et al.*¹² by a dimensionality analysis. The theory predicts that the angle derivative of the backscattered light intensity diverges to infinity at the exact backscattering direction for fractal dimensions less than three in contrast to the three-dimensional case. In the present study, however, the curves agree well with the theoretical ones for three-dimensional media within the experimental error. It shows that the multiple light scattering in the present porous glasses can be regarded as that in a uniform scattering medium in the spatial scale larger than l^* . The discrepancy between this result and the studies of energy transfer or x-ray scattering^{8,9} may be due to the difference in the spatial scale of the effectively probed volume.

We repeated the same measurement several times by changing the irradiation position for each sample. By the curve fitting as is shown in Fig. 1, we obtained the transport mean free path l^* for the four glass samples A, B, C, and D. The dependence of l^* on pore radius r is shown in Fig. 2 by open circles. Here the horizontal coordinate is the size parameter $kr = 2\pi r/\lambda$ with λ being the wavelength of light in the air, and the vertical coordinate is

taken as kfl^* in order to compensate for the small differences in the volume fractions f among the four samples. All the obtained values are almost on a straight line.

Also shown in the figure are results of calculation by three different methods under independent scattering approximation.¹³ In the first model, air spheres of a radius r are randomly distributed in glass. In the second one, straight cylinders of air with a radius r are randomly distributed in glass. In these two models, the radius r is taken to be the value of the mean pore radius of the sample glasses, and the volume fraction of air is set to the value of the corresponding sample. The transport cross section $\sigma^* = \langle \sigma(\omega)[1 - \cos(\omega)] \rangle$ of an air sphere and that of a cylindrical pore of a unit length in glass were calculated

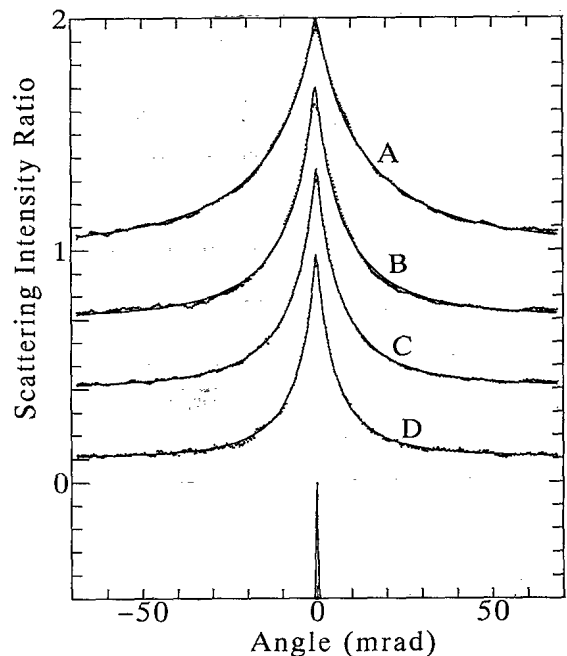


FIG. 1. Angular dependence of the backscattered light intensity for the porous glass samples A, B, C, and D (dots) together with the fitting curves (solid curves) based on the diffusion model for vector wave. The scattered light intensity is normalized to the incoherent scattering portion, and the curves for B, C, and D are shifted downward by 0.3 from the preceding one. The instrumental angle resolution curve is shown at the bottom.

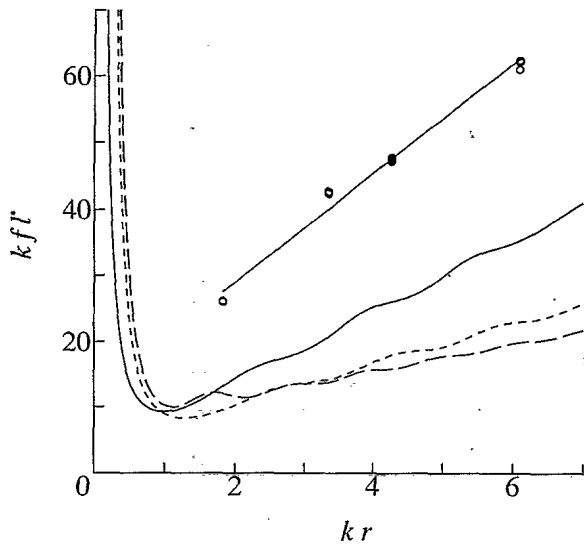


FIG. 2. Transport mean free path l^* (open circles) obtained by curve fitting to the backscattering peaks as are shown in Fig. 1. The short-dashed curve and the solid curve are the theoretical ones by the Mie scattering calculations for spherical holes of radius r in glass and for cylindrical pores of radius r in glass, respectively. The long-dashed curve is for calculated values by the form factor calculation.

according to the Mie theory,¹⁴ and, for the case of a cylinder, it was averaged over the random orientation of the cylinder. The transport mean free path l^* in the medium was calculated by

$$1/l^* = \sigma^* f / V, \quad (3)$$

where V is the volume of the sphere or the unit length cylinder. The spatial correlation between scatterers was not taken into account in the calculation although it has been shown to reduce the effective cross section for polystyrene latex.¹⁵ The refractive index of glass was set to 1.5 in the calculation. The calculated values of l^* are shown in Fig. 2 by a short-dashed curve for spherical holes and by a solid curve for cylindrical pores.

In the third method of calculation, the transport mean free path for randomly distributed spherical scatterers of air in glass was calculated by using the form factor of the sphere.^{14,16} Although this calculation is justified only for the weak scattering condition,

$$|n - 1|r \ll \lambda, \quad (4)$$

with n being the ratio of the refractive index of the host medium and that of the scatterer, it is worthwhile to compare the obtained result with those from the Mie scattering calculation, since the calculation is simple and convenient for further theoretical analysis.^{11,16} In this approximation,¹⁴ the transport cross section is expressed as

$$\sigma^* = 2\pi \left[\frac{k^2}{4\pi} \right]^2 (\epsilon_r - 1)^2 V^2 \int_0^\pi \sin\theta d\theta \frac{1 + \cos^2\theta}{2} \times (1 - \cos\theta) |F(\theta)|^2, \quad (5)$$

where V is the volume of the spheres, ϵ_r is the ratio of the dielectric constants (for the optical frequency) of the air and glass, k is the magnitude of the wave vector of light in glass, and $F(\theta)$ is the form factor of the sphere:

$$F(\theta) = \frac{3}{2kr \sin(\theta/2)} j_1[2kr \cdot \sin(\theta/2)]. \quad (6)$$

The function j_1 is the first spherical Bessel function. The calculated result is shown in the figure by a long-dashed curve. In spite of the weak-scattering approximation, the agreement of this result with that of the Mie scattering calculation is fairly good.

All the experimental data are almost on a straight line with a small offset from the proportional relation of the size parameter and kfl^* . Although the absolute values of the calculated curves do not agree with the experimental results, the almost linear dependence of l^* on the size parameter with small offsets is well reproduced. Especially, both the slope and the offset of the results of the Mie scattering calculation of spheres and cylinders agree very well with the experimental ones when they are multiplied by 2.7 and 1.8, respectively. The independent scattering approximation is not valid for the calculation of l^* in media with densely distributed scatterers such as our samples, where the volume fraction of pores ranges from 0.48 to 0.53. Therefore, the effect of spatial correlation among scatterers should be incorporated *via* the structure factor of the scatterer distribution to give reliable values,¹⁵ which may explain the factors of 2.7 or 1.8. Since the structure of the porous glasses can be expected somewhere between the two model structures considered here, the fact that either of the two models gave good agreement with the experimental data suggests that the transport properties of light in the actual porous glasses can be understood in the same theoretical framework. The result that the calculations based on the independent scattering approximation, which neglects the correlation effect, explain the experimental data very well shows that the wave vector dependence of the structure factors of the spatial distribution of scatterers in our samples is flat in the region of the scattering vector investigated in our experimental condition.

The nearly linear dependence of l^* on r are well reproduced in the calculated curves. It corresponds to the linear relation of the transport cross section and the geometric size of the scatterer for large scatterer sizes (geometric optics). As the radius r or the size of the scatterer is reduced from a size larger than the wavelength λ , the scattering changes from geometric optic scattering where $r > \lambda$, to the Mie scattering where $r \approx \lambda$, and to the Rayleigh scattering where $r < \lambda$. In the Rayleigh scattering region, l^* is proportional to $1/r^3$ in the independent scattering approximation, since the cross section is proportional to the square of the scatterer volume. Since the smallest size parameter studied in the present experiment is close to the crossover point of the r dependence of l^* from $l^* \propto r$ to $l^* \propto 1/r^3$, it is of interest to study the backscattering peaks from porous glasses by using samples with a smaller pore radius or using light with a longer wavelength.

III. TIME-OF-FLIGHT MEASUREMENTS

For the measurement of the temporal profile of a light pulse transmitted through the porous glass, output of a cw mode-locked dye laser was used as the incident light. The wavelength and the autocorrelation width of the dye laser pulses were 603.5 nm and 5 ps, respectively. The intensity of the pulse transmitted through the porous glass plate was detected by a synchroscan streak camera (Hamamatsu Photonics, M1955). The temporal width of the incident pulse observed by the streak camera was 21 ps, which was determined by the combination of the dye-laser pulse width, timing jitter of the pulse, and the time resolution of the streak camera. The observed temporal profiles of the pulses transmitted through the porous glass samples and the incident pulses are shown in Fig. 3 together with the theoretical fitting curves based on the diffusion model.⁴ The observed curves show very good agreement with the theoretical curves, and we can hardly see any deviations between them in Fig. 3. From curve fitting we obtained the diffusion constants D of light in the porous glass samples. The same measurement was repeated several times by changing the irradiation position on each porous glass sample, and the obtained values of D are shown in Fig. 4 by squares. Here the vertical coordinate is kfD/v_{glass} , where v_{glass} is the phase velocity of light in the glass which is $1/1.5$ times that of the light velocity in vacuum. The measured values of D scatter more for a larger pore radius r , since the temporal profile of the transmitted pulse decays faster for a larger r as is shown in Fig. 3, and the decay time approaches the resolution time. Like the transport mean free path l^* , the obtained diffusion constant D also has a nearly linear dependence on the size parameter kr .

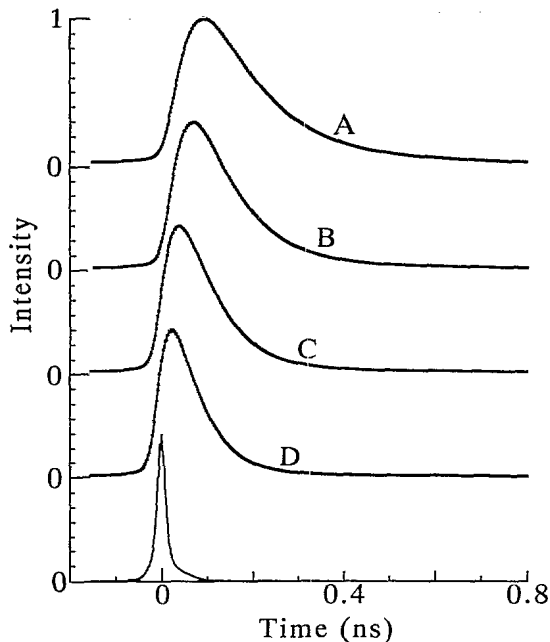


FIG. 3. Temporal profiles of transmitted pulses through the porous glass samples (presented by \times) together with the theoretical curves based on the diffusion model. The resolution curve of the measurement apparatus is shown at the bottom.

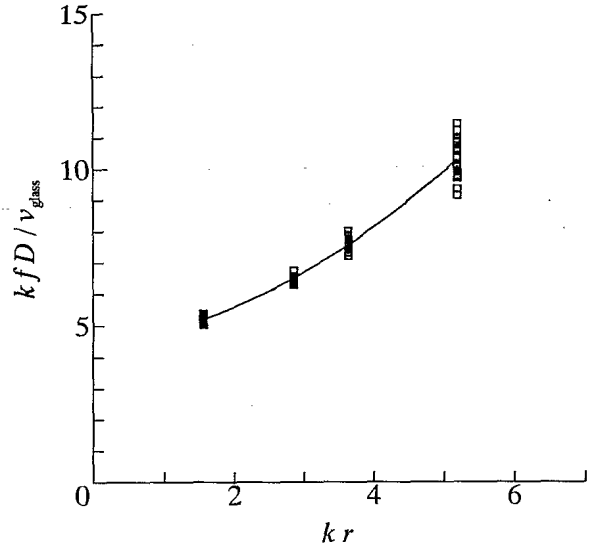


FIG. 4. Diffusion constant D obtained by curve fitting to the temporal profiles of the transmitted pulses through the porous glass samples.

In the Boltzmann picture of diffusion processes, where light is scattered by uniformly distributed point scatterers, l^* and D are related by the equation,

$$D = v_E l^* / 3, \quad (7)$$

where v_E is the transport velocity of light in the sample.⁵ The fact that both the obtained l^* (Fig. 2) and D (Fig. 4) have nearly linear dependence on r shows that the dependence of v_E on r is rather weak. From the obtained values of l^* and D , and the relation of Eq. (7), we derived the transport velocity of light v_E in the porous glasses, which is shown in Fig. 5. For this calculation, kfl^* was fitted to the first order and kfD/v_{glass} to the second order

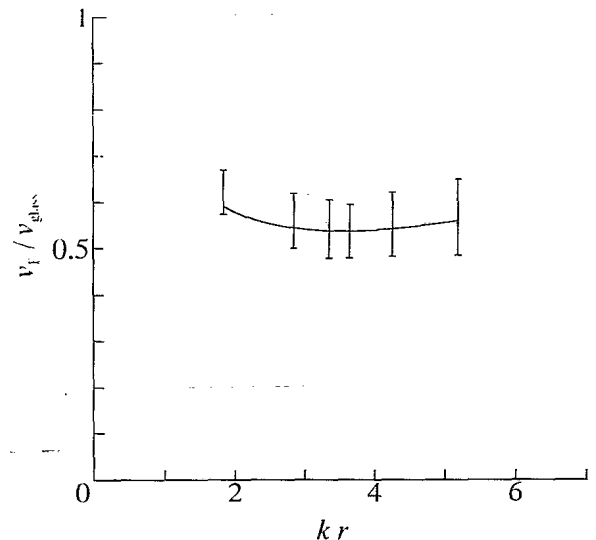


FIG. 5. Transport velocity v_E of light in the porous glass derived from the obtained transport mean free path l^* , diffusion constant D , and the relation of Eq. (7).

of kr . These fitting curves are shown in Figs. 2 and 4. In our porous glass samples the volume fractions of pore and glass are nearly equal, which leads to the expected value of v_E around the middle of v_{glass} and the light velocity in vacuum. The obtained v_E , however, is about 60% of v_{glass} through the measured range of kr with slight increase for small scatterers. This can be attributed to the phase shift of the scattered light wave in the sample^{5,17} with a high volume fraction f of scatterers and/or to the complicated network structure of the porous glass where light propagates mainly in the glass rather than in the pores by waveguide effect. The fact that no pronounced resonance structures are seen in the size parameter dependence of v_E suggests that the delay of propagation of light wave in our sample media should be attributed to the overall spatial distribution of scatterers rather than to each scatterer. Although similar result was obtained by the study of microwave diffusion in random ensembles of polystyrene spheres,¹⁸ and light diffusion through titania particles,⁵ the scatterer size dependence of the transport velocity was not studied in these reports.

IV. CONCLUSION

The shape of the backscattering peak and the temporal profile of the transmitted pulse from porous glasses in the present measurement showed very good agreement with the theoretical result of the diffusion model in three-dimensional media. By curve fitting we obtained the values of l^* , D , and v_E of our porous glass samples. The microscopic structure of the porous glass is reflected in the values of l^* , D , and v_E . The understanding of these values needs more detailed information on the microscopic structure of the porous glass and more precise analysis of light scattering. The multiple scattering of light in our porous glass samples can be regarded as that in uniform scattering media in the scale larger than the transport mean free path l^* . The pore radius dependence of the transport mean free path l^* could be explained well by a calculation based on the independent scattering approximation. The transport velocities of light in the media calculated from the obtained values of l^* and D were about 60% of the value in the bulk glass.

¹M. P. van Albada and A. Lagendijk, Phys. Rev. Lett. **55**, 2692 (1985).

²P.-E. Wolf and G. Maret, Phys. Rev. Lett. **55**, 2696 (1985).

³G. H. Watson, Jr., P. A. Fleury, and S. L. McCall, Phys. Rev. Lett. **58**, 945 (1987).

⁴J. M. Drake and A. Z. Genack, Phys. Rev. Lett. **63**, 259 (1989).

⁵M. P. van Albada, B. A. van Tiggelen, A. Lagendijk, and A. Tip, Phys. Rev. Lett. **66**, 3132 (1991).

⁶M. Rosenbluh, I. Edrei, M. Kaveh, and I. Freund, Phys. Rev. A **35**, 4458 (1987).

⁷S. Etemad, R. Tompson, M. J. Andrejko, S. John, and F. C. MacKintosh, Phys. Rev. Lett. **59**, 1420 (1987).

⁸U. Even, K. Rademann, J. Jortner, N. Manor, and R. Reisfeld, Phys. Rev. Lett. **52**, 2164 (1984).

⁹A. Höhr, H. B. Neumann, P. W. Schmidt, P. Pfeifer, and D.

Avenir, Phys. Rev. B **38**, 1462 (1988).

¹⁰F. C. MacKintosh and S. John, Phys. Rev. B **37**, 1884 (1988).

¹¹K. J. Peters, Phys. Rev. B **46**, 801 (1992).

¹²E. Akkermans, P. E. Wolf, R. Maynard, and G. Maret, J. Phys. (Paris) **49**, 77 (1988).

¹³H. C. van de Hulst, *Light Scattering by Small Particles* (Dover, New York, 1981).

¹⁴A. Ishimaru, *Wave Propagation and Scattering in Random Media* (Academic, New York, 1978), Vols. 1 and 2.

¹⁵P. E. Wolf, G. Maret, E. Akkermans, and R. Maynard, J. Phys. (Paris) **49**, 63 (1988).

¹⁶F. C. MacKintosh and S. John, Phys. Rev. B **40**, 2383 (1989).

¹⁷G. Cwilich and Y. Fu, Phys. Rev. B **46**, 12 015 (1992).

¹⁸N. Garcia, A. Z. Genack, and A. A. Lisyansky, Phys. Rev. B **46**, 14 475 (1992).